Chemical Engineering Science, 1976, Vol. 31, pp. 373–380. Pergamon Press. Printed in Great Britain

ACIDIZATION—IV

EXPERIMENTAL CORRELATIONS AND TECHNIQUES FOR THE ACIDIZATION OF SANDSTONE CORES

K. LUND† and H. S. FOGLER‡
Department of Chemical Engineering, University of Michigan, Ann Arbor, MI 48104, U.S.A.

and

C. C. McCUNE and J. W. AULT
Chevron Oil Field Research Company, La Habra, CA 90631, U.S.A.

(*Received* 28 *August* 1974; *accepted in revised form* 10 *October* 1975)

Abstract—The experimental variables that affect the acidization of sandstone cores in a permeameter are discussed. It was found that as HCl/HF acid mixtures are injected into porous sandstone cores a reaction front between selective minerals and the acid is formed. This reaction front and a corresponding permeability front move through the core with a constant axial velocity. The time for the permeability front to move through the core is defined as the break-through time. The breakthrough time is directly proportional to the core length but inversely proportional to the HF acid concentration and the rate of injection.

INTRODUCTION

In our previous papers[1–3] we reported the kinetics of the reactions between HCl and HCl/HF acid mixtures with various minerals (e.g. calcite, dolomite, albite, and microcline), which are commonly found in sandstone. In this paper we shall report experimental techniques used to study and identify the important parameters in the flow and reaction of acids in porous sandstone. In addition, experimental correlations will be presented to describe the movement of the permeability front through a linear sandstone core.

The flow of a fluid through a porous media is described by Darcy's law (in one dimension):

$$q = -\frac{k}{\mu}\frac{dp}{dx} \tag{1}$$

where

q = rate of fluid flow through a unit area; ml/sec/sq cm,
k = permeability; Darcies,
μ = viscosity; centipoise,
$\frac{dp}{dx}$ = pressure gradient; atm/cm.

Many attempts have been made to find relationships between the permeability and the other properties of the porous media. Although empirical correlations have been found relating the permeability with porosity, pore size distribution, or grain size distribution it is clear that they can only have limited validity.

A better understanding of the porous media may possibly be arrived at by proposing suitable microscopic models and computing macroscopic properties of the porous media from these models. In nearly all of the microscopic models the pores are approximated as capillary tubes. In the simplest model the pore space in a core of porous media is treated as a bundle of straight, parallel capillaries of uniform radius running all the way through the porous core. Most often a porous media will have a distribution of pore sizes, and this may also be included in the model by introducing a pore size distribution function[4]. The model may be refined by assuming the porous core to be divided into thin sections (normal to the direction of flow) and the flow of fluid exiting from each section to be fully mixed before entering the next section[5–11]. Schechter[5–9] applied this pore model to acidization by following the pores in each section as they grow and collide. The Schechter model was tested experimentally[6, 8–10] on well-ordered porous media having a narrow pore size distribution with good results. The increase in the permeability is mainly a result of the growth of the larger pores.

An inherent weakness of a model based on a capillary description lies in the ill defined nature of a pore size distribution function. The three dimensional porous network is described by a pore size distribution only as a function of the pore radius. No information on the shape, length, or connections of the pores is included. In addition, measurement of the larger pores, which are believed to be the most important during acidization, are determined with the least accuracy[12]. A further complication arises when a porous media such as sandstone having a heterogeneous solid matrix is to be described.

MATRIX ACIDIZATION OF SANDSTONE

The porous formation rock, sandstone, consists of a mass of angular mineral grains of widely different sizes

†Present address: Norsk Hydro, Bygdøy Alle 2, Oslo, Norway.
‡To whom correspondence should be addressed.

and composition. Quartz is the main mineral constituent of sandstone although considerable amounts of other minerals such as feldspars, clays, and carbonates may be present. The chemical composition of different grains of the same mineral species may show quite a variance since the chemical composition of a mineral may vary within set limits.

A full microscopic description of a sandstone therefore not only necessitates a pore size but also a mineral distribution function. This would be difficult to obtain and there is little chance that such an approach will give results of practical value for acidization. For systems as complex as this, a better approach would be to describe the system by a macroscopic model that may contain parameters which lump information about the geometry, the flow, and the reactions within the porous media. Some of these parameters must be determined experimentally for each sandstone in question, whereas others may have general validity.

As a basis for proposing and substantiating a model for the acidization of sandstone, a quartzite sandstone was investigated in detail both by experiment and theory. The experimental part of this investigation is described in the present paper, whereas the development of a model is covered in a following paper.

EXPERIMENTAL

Quartzite sandstone samples used in this investigation were collected from an outcrop in the Chico Martinez Creek, Kern Co., California. Microscopic examination of a thin section of the sandstone showed it to be a feldspathic quartzite composed of quartz grains, feldspars, minor amounts of quartzite rock fragments, small amounts of altered biotite, interstial clay-chloritic material and scattered heavy mineral grains. The grains are very poorly sorted and range from fine to very coarse in size. The grains are subangular to angular and ragged in shape.

X-ray diffraction analysis shows the average mineralogical composition of this sandstone to be 80·3 wt% quartz, 5·9 wt% plagioclase, 11·6 wt% potassium feldspar, and 2·2% illite and kaolinite.

The acidization of the sandstone cores was carried out in a high pressure, high temperature permeameter (see Fig. 1); a full description of the apparatus and its operation has been reported[13]. Mixtures of hydrofluoric and hydrochloric acid were pumped at constant rates through 1 in. dia. cores. The permeability of the core was measured as a function of time, and samples of the effluent acid were collected[14]. The strength and flow rate of the acid mixture, the length of the core, and the volume of acid injected were varied in the series of experiments. After each experiment the core was retrieved and sectioned with a diamond saw. Parameters such as porosity, pore size distribution, mineral concentrations and permeability were measured for several sections. Two series of acidization experiments were conducted, and the average properties of the sandstone were only slightly different in the two series. The properties of the sandstone and the complete experimental data from the two series of acidization experiments are given elsewhere[14].

In mounting a core for an acidization experiment (see Fig. 2), the core was first coated with an epoxy adhesive (on the cylindrical surface only) and then sandwiched between 100 mesh Hastalloy screens and two end-plates. Heat shrinkable Teflon tubing was shrunk over this assembly, which was then mounted rigidly inside a steel tube. The steel tube with the sandstone core was then mounted in a Hassler-type cell and a selected overburden pressure (5000 psig) was applied on the core by pressurizing the Teflon Hassler sleeve with white oil.

While the overburden pressure enables one to stay within the design limitations of the permeameter, it tends to reduce the permeability of the sandstone cores. To determine if the overburden pressure affected the results,

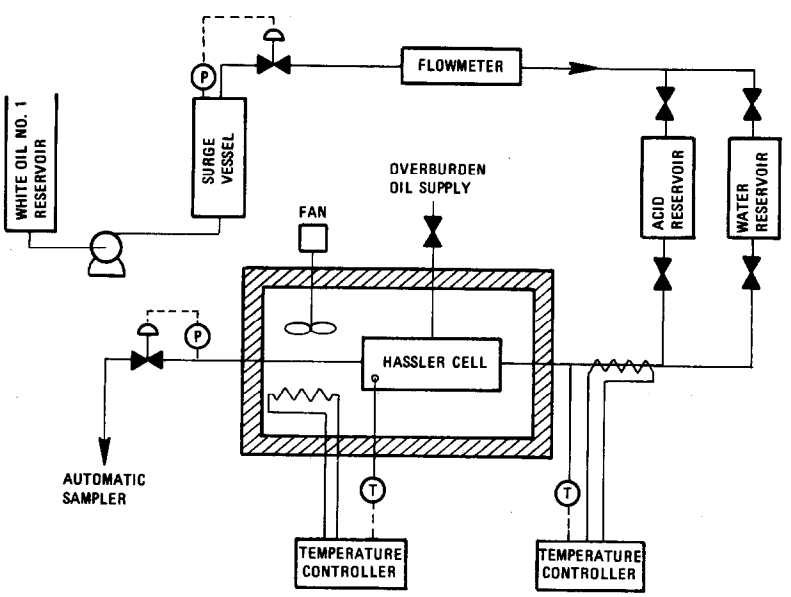

Fig. 1. Schematic of permeameter.

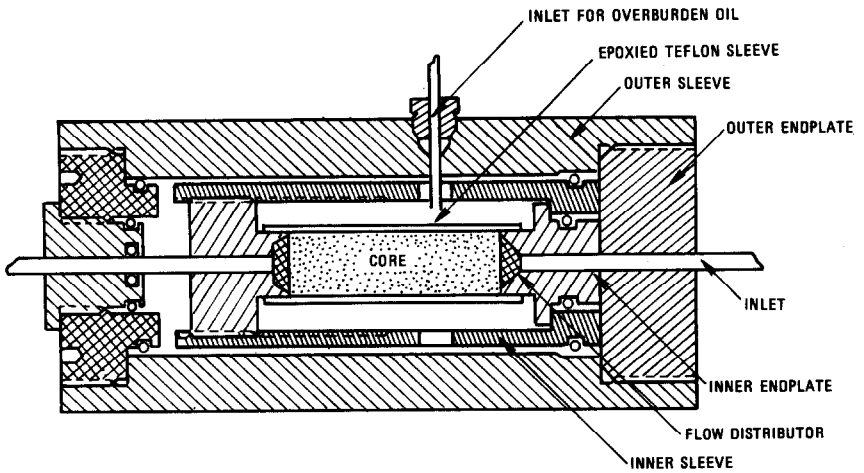

Fig. 2. Schematic of Hassler cell.

some experiments had to be performed without an applied overburden pressure. Except for the direct effect on the permeability, control experiments showed the behavior of the core during the acidization to be unaffected by overburden pressure. Separate heaters and temperature controllers on the Hassler cell and on the upstream flow lines maintained a constant temperature during the flow experiment (i.e. within 2–3°F).

The procedure followed in the acidization experiments, was that a core was first vacuum saturated with distilled water and then flooded with distilled water to measure the initial permeability. The temperature of the core, the overburden pressure, and the flow-rate were adjusted until the desired values were reached. When the differential pressure across the core had remained constant for about 0·5 hr, injection of the acid mixture through the core and sampling of the effluent acid were begun. After a significant increase in the permeability of the core (*at least* 3-fold) the flow of acid was stopped, and distilled water was again injected through the core.

After each acidization experiment a series of analyses was performed on the core and the effluent acid. The effluent acid was analyzed for Na, K, Ca, Mg, Al, and Si with a Perkin–Elmer model 303 atomic absorption spectrophotometer. The permeability, porosity, pore size distribution, and the concentration of minerals in the core (or segment of a core) were also determined. Permeability was measured in a permeameter, porosity in a Kobe porosimeter[15], and pore size distribution by mercury injection. The concentration of minerals in the sandstone core was determined by X-ray diffraction.

DISCUSSION OF RESULTS

Permeability changes during acidization

The permeability of a sandstone is often sensitive to the ionic content of the aqueous solution flowing through it and in some instances the permeability may decrease drastically and irreversibly. This reduction in permeability (i.e. damage) is caused by the interaction of clays in the sandstone[16, 17] with the flowing fluid.

For a sandstone core undergoing acidization the plot of the permeability k as a function of time, t, has a characteristic shape. This is illustrated in Figs. 3 and 4 where the permeability ratio, K/K_I, is plotted as a function of the dimensionless injection time, τ. Here K_I is the initial permeability of the core and the number of pore volumes injected, θ, is defined as:

$$\theta = t/\tau \tag{2}$$

$$\tau = L\phi/q \tag{3}$$

where L is the length of the core; cm, and ϕ is the porosity.

These figures show that during the first part of the acidization, the average permeability of the core remains either essentially constant or it may perhaps even decrease somewhat. This behavior is a result of the interaction of the acid solution with the clays (illite and kaolinite) and other fines causing a reduction of permeability in a section of the core. When the acid has dissolved most of the readily dissoluable minerals in the larger pores of the core, the permeability increases rapidly. The time period necessary to achieve this result may be called the ***breakthrough time***, t_b. That is, the breakthrough time is the time necessary to inject acid through the core in order to start to significantly increase the permeability of the core. In the last phase of the acidization, the permeability of the core becomes fairly constant again. The structural strength of the sandstone will be decreased by the acidization and the core may partially collapse under the influence of the overburden pressure. The permeability of the core will generally be lowered if this occurs. The actual value of the permeability in the last stage will be quite dependent on the number of the larger pores present in the sample and the degree of collapse that has taken place during the acidization.

During the acidization the (local) permeability $k(x, t)$ at any point in the core will be a function of time and position. The average permeability $K(t)$ of the core at any time is given by:

$$K(t) = L \Big/ \int_0^L \frac{dx}{k(x,t)} \tag{4}$$

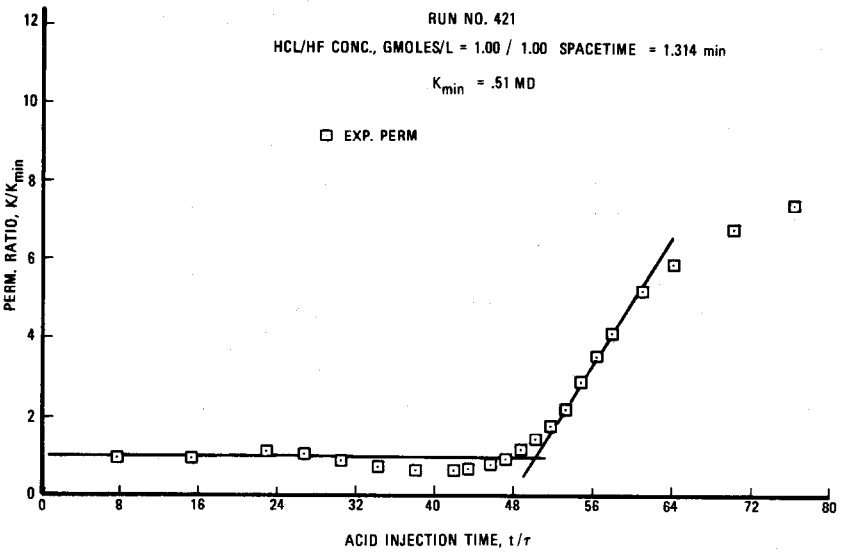

Fig. 3. Permeability of a core during acidization vs dimensionless time.

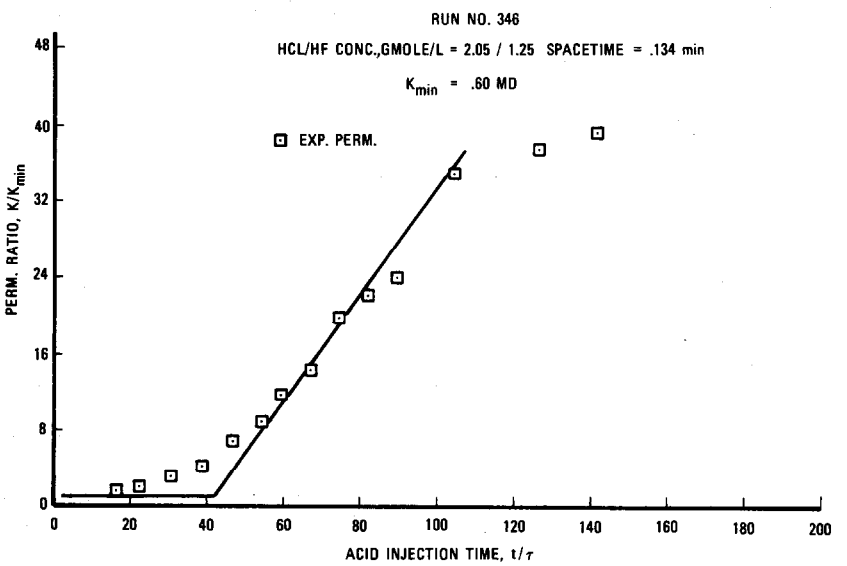

Fig. 4. Permeability of a core during acidization vs dimensionless time.

where L is the length of the core. From this calculation it is clear that the section of the core having a low permeability will have a dominant effect on the value of the average permeability.

To obtain a better understanding of the variation of the local permeability during acidization some acidized cores were cut (normal to the direction of flow) into 0·5 or 1 in. core segments and the permeability of the segments was measured. The ratio of the local permeability to the initial core permeability is shown in Fig. 5 as a function of axial position in the core for runs 344, 434, 437 and 438. The axial distance is measured from the up-stream face. The acid injection time and concentration of acid were varied while the superficial velocity of the acid was approximately the same for this set of experiments (0·20–0·26 cm/min). After acidization the average permeability of the cores in the experiments R434 and R438 was significantly higher than the initial permeability (i.e. breakthrough had occurred), whereas this was not the case for R344 and R437. The two latter cores show severe reduction of the permeability in part of the core as a result of damage. At permeability ratios larger than 1·0 we observe from Fig. 5 that the permeability profiles have approximately the same shape and that the location of each profile is simply determined by the amount of acid injected into the core. Since the acid was injected at a constant rate in the experiments, this result implies that the zone of rapidly changing permeability may be considered as a front which moves through the porous media with a constant velocity.

Analysis of the effluent acid

In several of the experiments the effluent acid from the core was collected and analyzed for Na, K, Ca, Mg, Al and Si. In Figs. 6 and 7 the results of the analysis of a typical experiment, R341, is plotted as a function of a

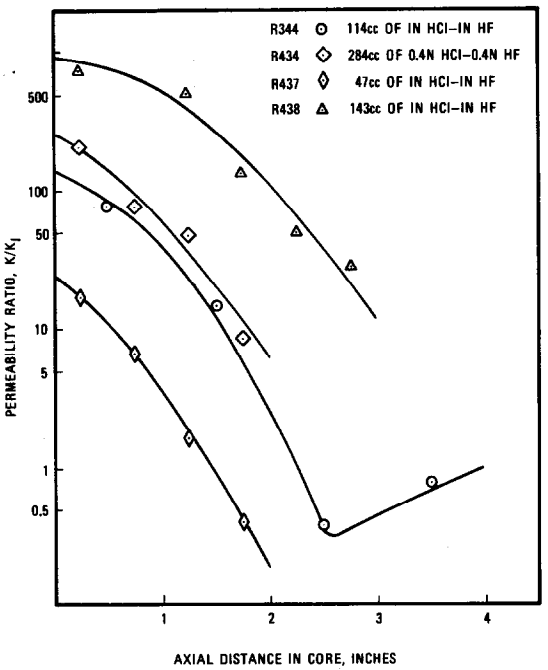

Fig. 5. Permeability profile in cores which have undergone acidization.

dimensionless injection time, θ. In run 341 an acid mixture with a concentration of 1·4 wt% HCl and 0·8 wt% HF was injected at a rate of 0·22 cm^3/sq cm/min through the core. As previously mentioned, cores from the same sandstone may not have identical mineralogical composition and the individual minerals may vary in composition. Consequently the trends for the composition of the effluent acid can be expected to show some variation and it is only possible to relate the content of the different elements in the acid to the dissolution of specific minerals in the core in a qualitative or at best, semi-quantitative manner. As the acid enters the pores of the core, the dissolving minerals will compete for the reactants in the acid mixture. The mineral for which the product of the dissolution rate and accessible surface area is the greatest will be dissolved preferentially. The relatively large concentration of the elements Ca and Mg in the first sample collected suggests that carbonates are being dissolved first as one would expect. In samples at subsequent times, the concentrations of K, Na, Al and Si reach a maximum and then slowly decline. The preferential dissolution of the aluminosilicates such as feldspars and clays is taking place and their dissolution rates are similar.

In a previous paper [3] we discussed the dissolution of aluminosilicates in hydrochloric–hydrofluouric acid mixtures and the equilibria in which aluminum and silicon participate. Since the concentration of Na, K, Ca, Mg, Al and Si in the effluent acid are known from the chemical analysis, then it is possible to determine the approximate concentration of H^+ and HF in the effluent acid by solving the system of non-linear algebraic equations describing the equilibria in the ionic solution.

In Table 1 the results of this type of calculation for the second sample of effluent acid from R346 are given. The calculated concentration of HF in the effluent acid is shown as a function of time in Figs. 7 and 8 for experiments R341 and R346 respectively. The rate of acid injection through the core was approximately nine times larger in R346 than in R341, and the reaction front of the hydrofluoric acid in the core should be sharper in the latter experiment. When most of the readily dissoluble and accessible minerals in the core have been removed by the acid, the concentration of HF in the effluent acid should increase more rapidly in R341 as compared with R346. From the figures we observe this to be true. Most often the concentration of H^+ varies only slightly (see Fig. 8) and we note that the H^+ concentration may actually increase due to the release of H^+ from HF in some of the homogeneous reactions.

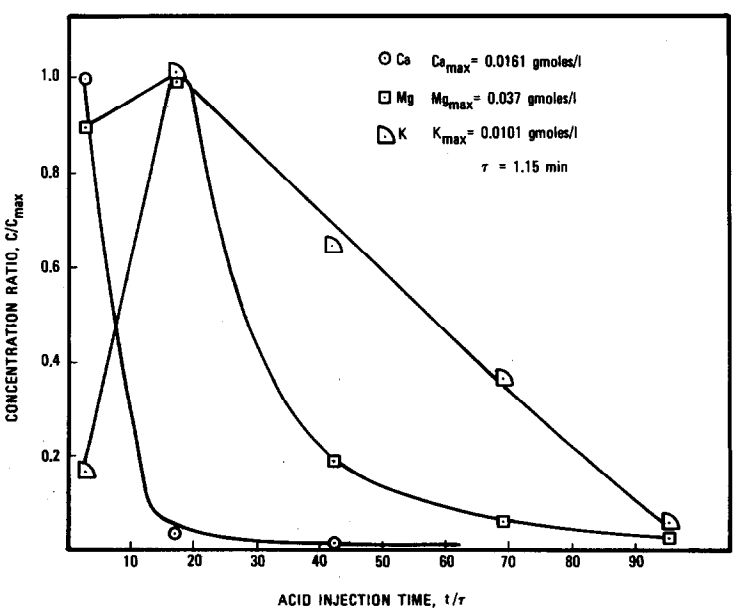

Fig. 6. Composition of effluent acid from R341 as a function of dimensionless time.

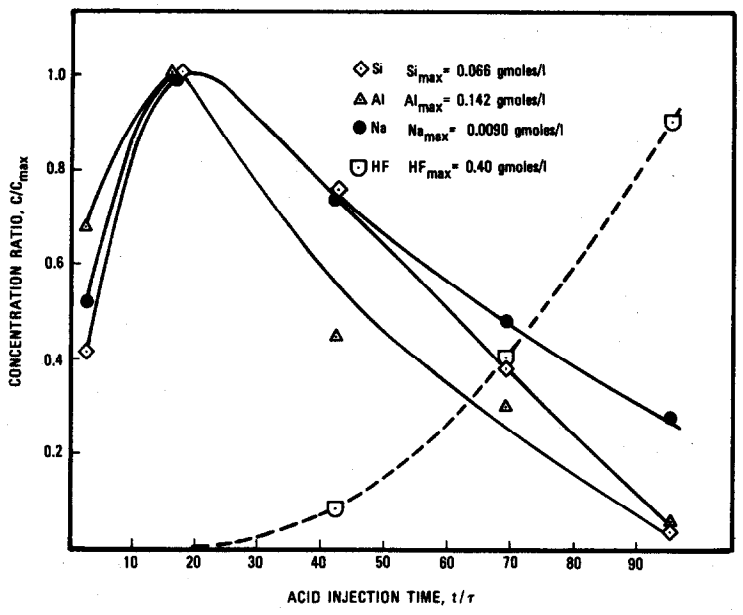

Fig. 7. Composition of effluent acid from R341 as a function of dimensionless time.

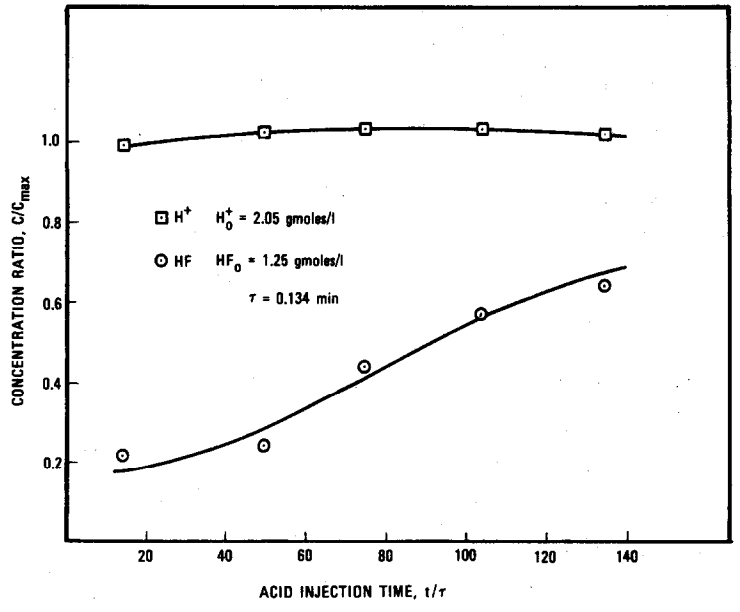

Fig. 8. Calculated concentrations of HF and CHl in the effluent acid from R346.

Table 1. Measured and calculated concentrations of sample 2 of effluent acid from R346 (in mole/l.)

Initial acid concentration: $[HCl_o] = 2.05$; $[HF_o] = 1.25$		
Concentrations measured by atomic absorption spectometer:		
$[Na^+] = 0.0207$	$[Ca^{++}] = 0.00195$	
$[K^+] = 0.0081$	$[Al_t] = 0.075$	
$[Mg^{++}] = 0.0070$	$[Si_t] = 0.155$	
Concentrations calculated from the equilibrium relationships:		
$[Al^{3+}] = 0.21 \times 10^{-4}$	$[AlF_3] = 0.031$	$[AlF^{3-}] = 0.30 \times 10^{-8}$
$[AlF^{2+}] = 0.0033$	$[AlF_4^-] = 0.0019$	$[SiF_4] = 0.0060$
$[AlF_2^+] = 0.039$	$[AlF_5^{=}] = 0.91 \times 10^{-5}$	$[SiF_5^-] = 0.149$
$[SiF_6^{=}] = 0.82 \times 10^{-4}$	$[Cl^-] = 2.05$	
$[H^+] = 2.11$	$[F^-] = 0.95 \times 10^{-4}$	
$[HF] = 0.30$		

Petrographic analysis of sandstone cores

The identity and concentration of the crystalline minerals in the porous media were determined by X-ray analysis with aluminum added as an internal standard to quantify the results (called an aluminum petrolog). The acidization studies on sandstone were carried out by performing two series of experiments. The sandstone cores for the two series were cut from two different blocks of the same sandstone (quartzite) and they do show some differences, although minor, in composition as determined by X-ray diffraction:

The analysis also indicated a small amount of amorphous material to be present (1–3 wt%) but due to the

method of determination at least part of this may be analytical error. The results of the analysis on the center portion of the cores after acidization in runs 341 and 342 are also shown in Table 2. For both of these cores the injection of acid was continued until after breakthrough had occurred. As expected the analyses show the feldspars and the clays to dissolve preferentially. If we assume the quartz to be inert during acidization a mass balance on the feldspars and clays shows that approximately one third of these minerals are being dissolved.

Porosity and pore size distribution measurements

The porosity, ϕ, of the quartzite was measured with a Kobe porosimeter[15], and the following values were found before acidization:

Series 1 (R341–R348) $\phi = 9{\cdot}9\%$
Series 2 (R421–R478) $\phi = 12{\cdot}0\%$.

The accuracy of the measurement was approx. ±1·0%. After most of the experiments the porosity of the acidized core (either whole or sectioned) was measured. Generally it was found, that although dramatic increases in the permeability had occurred, the porosity had changed only by a small amount. This is illustrated by comparing the porosities of the sectioned cores from the experiments R434, R437 and R438 given in Table 3 with their permeability profiles shown in Fig. 5.

The porosities of the core sections (0·5 in. long) are listed in order of the direction of flow. In R437 the acidization was stopped before breakthrough had occurred. The increase in the permeability for the given change in porosity is substantially larger than what has been predicted by the capillary models described earlier[4–11]. This result illustrates that the main mechanism for the increase of the permeability is probably not the uniform dissolution of all of the pore walls but rather the selective removal of mineral debris, exposed mineral grains, and constrictions in the larger pores.

The change in the porosity of a core may also be computed from the chemical analysis of the effluent acid, since the change in pore volume is equal to the mass dissolved from the core divided by the average sand grain density (2·62 g/cm^3). For example, Table 4 is a list of some of the calculated and measured porosities. In general the

Table 2. Petrographic analysis of unacidized and acidized cores

	Unacidized Series 1 (R341-R348) Weight %	Unacidized Series 2 (R421-R478) Weight %	Acidized Run 341 Weight %	Acidized Run 342 Weight %
Quartz	79.4	82.3	85.1	84.9
Plagioclase	6.6	5.1	4.8	5.8
K-feldspar	12.5	10.7	9.6	8.8
Kaolinite	0.8	0.8	-	-
Illite	1.7	1.1	0.5	0.5

Table 3. Porosity measurements of acidized cores

Experimental Run		Mean axial position of sample in core (cm) 0.63	1.90	3.17	4.44	5.71	6.98
R434	ϕ(%) =	19.5	15.4	15.7	15.5		
R437	ϕ(%) =	15.7	15.4	14.1	14.0		
R438	ϕ(%) =	17.8	16.1	15.8	16.0	17.0	19.4

Table 4. Core porosities computed from chemical analysis of the effluent acid

Experiment	Computed	Measured
R436	ϕ = 14.5%	14.7%
R437	ϕ = 13.4%	avg. 14.8%
R440	ϕ = 22.5%	25.1%

calculated porosities are somewhat lower than the measured ones and this may be due to several reasons other than measurement errors; (1) some porosity may be inaccessible to the porosimeter; (2) precipitates formed in the core during the acidization may dissolve during the post acidization injection of distilled water and thereby increase the porosity by an unmeasured amount; (3) solids may be washed out of the core; and (4) some of the effluent acid may be lost through leaks and during the change of sample bottles. However, there is still good agreement between the measured and calculated porosities.

The pore size distributions of various samples before and after acidization were obtained by use of a mercury porosimeter[14]. Primarily, the diameter of the larger pores are increased by the acidization but on the other hand the growth of a few larger pores does not dominate the acidization as has been reported for the acidization of limestone cores[5].

Experimental breakthrough correlation

Earlier it was proposed in connection with Fig. 5 that in a sandstone core undergoing acidization a zone of rapidly changing permeability may be considered as a front which moves through the core with a characteristic velocity. Furthermore, the position of the front seemed to be proportional with the amount of acid injected, i.e.

$$X_f R = qC_0 t \tag{5}$$

where C_0 is the HF concentration in the acid mixture (mole/cm^3); q, the rate of acid injection per unit area normal to direction of flow (cm/min); t, the injection time (min); X_f, the position of the front from the up-stream face of the core (cm); and R, the constant of proportionality.

If we define the time, t_b, at which breakthrough occurs for a core of length L as the intersection between the lines $K = K_I$ and the asymptote to that part of the permeability vs time curve where the permeability increases rapidly (see Figs. 3 and 4), then eqn (5) becomes:

$$qC_0 t_b / L = R \tag{6}$$

where L is the length of the core (i.e. $L = X_f$), and R, the characteristic constant of the porous media. An average value of R may be calculated for all of the experiments:

$$R = 0{\cdot}0046 \text{ moles/cm}^3$$

In Fig. 9 the experimentally measured breakthrough times are compared with those we may calculate from eqn (6) for $R = 0{\cdot}0046$ moles/cm^3. When we consider the complexity of the porous media and the simple form of eqn

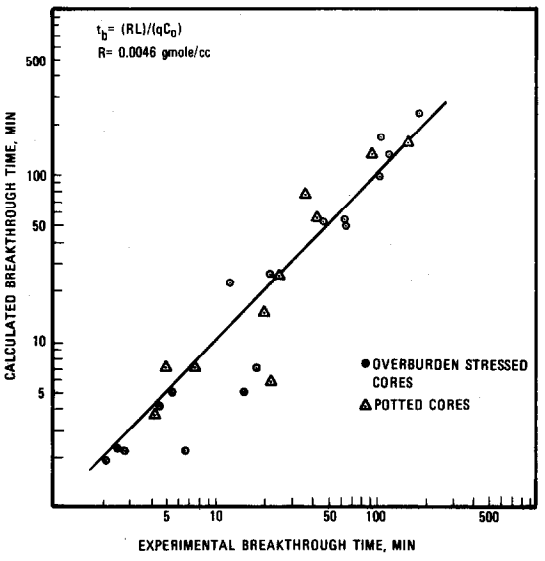

Fig. 9. Calculated breakthrough time from correlation vs experimental breakthrough time.

(6), the agreement between data and correlation is surprisingly good. The four experimental points that deviate significantly from the correlation were measured for short cores (1/2 in. and 1 in.) and high acid flowrates (approx. 2·5 cm^3/sq cm/min). Under these conditions we would not expect the correlation to be valid since a sharp permeability front will not be established in the core. In some of the acidization experiments the cores were stressed by an overburden pressure, whereas, in other experiments this was not the case. From Fig. 9, one observes no difference in breakthrough time due to this experimental procedure.

Equation (6) together with the other experimental results suggest that during the acidization fronts of strongly changing permeability and hydrofluoric acid concentration move through the core with a constant characteristic velocity. The constant, R, should then simply be a measure of the amounts of solids to be dissolved per unit bulk volume of the sandstone. During the acidization the acid mixture dissolves about a third of the feldspars and clays in the core. The concentration of these solids (lumped together as feldspar) is $1{\cdot}5 \times 10^{-3}$ moles per unit volume of quartzite. Taking the stoichiometric coefficient to be 15 moles HF per mole feldspar [14], one may estimate R to be:

$$R = (\tfrac{1}{3})1{\cdot}5 \times 10^{-3} \times 15 = 7{\cdot}5 \times 10^{-3} \text{ moles/cm}^3. \quad (7)$$

This result is in good agreement with the experimental data.

CONCLUSIONS

(1) In the acidization of sandstone cores the HF/HCl acid mixture selectively dissolves the more reactive minerals such as the feldspars and clays. The α-quartz does not react to any appreciable extent.

(2) The dramatic increase in the permeability of a sandstone core undergoing acidization is probably due to the selective dissolution of the reactive minerals which are present in the larger pores in the form of exposed grains and debris.

(3) The dissolution of the minerals in the core produces a change in the local permeability which travels as a front with a constant axial velocity through the cylindrical core.

(4) The time it takes the permeability front to travel through the core may be called the breakthrough time. The breakthrough time is proportional to the core length and inversely proportional to the HF acid concentration and the rate of injection.

NOTATION

C_0 initial (inlet) concentration of HF acid, mole/cm^3
dp/dx pressure gradient, atm/cm
K average permeability, Darcy
k local permeability, Darcy
L core length, cm
q rate of fluid flow, cm^3/cm^2/min
R breakthrough model number (defined by eqn (6)), mole/cm^3
t time period of acid injection, min
t_b breakthrough time, min
V_f velocity of permeability front, cm/min
x axial position in core, cm
X_f axial position of permeability front, cm

Greek symbols

θ dimensionless time, t/τ
μ fluid viscosity, centipoise
ϕ porosity
ν stoichiometric coefficient
τ space time (time to fill one pore volume of core), min

REFERENCES

[1] Lund K., Fogler H. S. and McCune C. C., *Chem. Engng Sci.* 1973 **28** 691.
[2] Lund K., Fogler H. S., McCune C. C. and Ault J. W., *Chem. Engng Sci.* 1975 **30** 825.
[3] Fogler H. S., Lund K. and McCune C. C., *Chem. Engng Sci.* 1975 **30** 1325.
[4] Rowan G., *J. Inst. Pet.* 1959 **45** 321.
[5] Schechter R. S. and Gidley J. L., *A.I.Ch.E.J.* 1969 **15** 339.
[6] Guin J. A., Ph.D. Thesis, University of Texas (1969).
[7] Guin J. A. and Schechter R. S., *Soc. Pet. Engr. J.* 1971 **11** 390.
[8] Guin J. A., Schechter R. S. and Silberberg I. H., *Ind. Engng Chem. Fund.* 1971 **10** 50.
[9] Sinex W. E., Schechter R. S. and Silberberg I. H., *Ind. Engng Chem. Fund.* 1972 **11** 205.
[10] Guin J. A. and Glover M. C., 74 *National Meeting of A.I.Ch.E.* 52 d New Orleans, March (1973).
[11] Williams B. B. and Whiteley M. E., *Soc. Pet. Engr. J.* 1971 **11** 306.
[12] Scheidegger A. E., *The Physics of Flow Through Porous Media.* Macmillan, New York (1957).
[13] Farley, J. T., Miller B. M. and Schoettle V., *J. Pet. Tech.* 1970 **22** 433.
[14] Lund K., Ph.D. Thesis, University of Michigan (1974).
[15] Beeson C. M., *Pet. Trans. AIME* 1950 **189** 313.
[16] Mungan, N., *J. Pet. Tech.* 1965 **17** 1449.
[17] Smith C. F. and Hendrickson A. R., *J. Pet. Tech.* 1965 **17** 215.